

Search for pair-production of strongly-interacting particles
decaying to pairs of jets in $p\bar{p}$ collisions at $\sqrt{s} = 1.96$ TeV

T. Aaltonen,²¹ E. Albin,⁵⁷ S. Amerio,⁴⁰ D. Amidei,³² A. Anastassov^x,¹⁵ A. Annovi,¹⁷ J. Antos,¹² G. Apollinari,¹⁵ J.A. Appel,¹⁵ T. Arisawa,⁵³ A. Artikov,¹³ J. Asaadi,⁴⁸ W. Ashmanskas,¹⁵ B. Auerbach,² A. Aurisano,⁴⁸ F. Azfar,³⁹ W. Badgett,¹⁵ T. Bae,²⁵ A. Barbaro-Galtieri,²⁶ V.E. Barnes,⁴⁴ B.A. Barnett,²³ P. Barria^{hh},⁴² P. Bartos,¹² M. Bauc^{ff},⁴⁰ F. Bedeschi,⁴² S. Behari,¹⁵ G. Bellettini^{gg},⁴² J. Bellinger,⁵⁵ D. Benjamin,¹⁴ A. Beretvas,¹⁵ A. Bhatti,⁴⁶ K.R. Bland,⁵ B. Blumenfeld,²³ A. Bocci,¹⁴ A. Bodek,⁴⁵ D. Bortoletto,⁴⁴ J. Boudreau,⁴³ A. Boveia,¹¹ L. Brigliadori^{ee},⁶ C. Bromberg,³³ E. Brucken,²¹ J. Budagov,¹³ H.S. Budd,⁴⁵ K. Burkett,¹⁵ G. Busetto^{ff},⁴⁰ P. Bussey,¹⁹ P. Butti^{gg},⁴² A. Buzatu,¹⁹ A. Calamba,¹⁰ S. Camarda,⁴ M. Campanelli,²⁸ F. Canelli^{oo},^{11,15} B. Carls,²² D. Carlsmith,⁵⁵ R. Carosi,⁴² S. Carrillo^m,¹⁶ B. Casal^k,⁹ M. Casarsa,⁴⁹ A. Castro^{ee},⁶ P. Catastini,²⁰ D. Cauz,⁴⁹ V. Cavaliere,²² M. Cavalli-Sforza,⁴ A. Cerri^f,²⁶ L. Cerrito^s,²⁸ Y.C. Chen,¹ M. Chertok,⁷ G. Chiarelli,⁴² G. Chlachidze,¹⁵ K. Cho,²⁵ D. Chokheli,¹³ M.A. Ciocci^{hh},⁴² A. Clark,¹⁸ C. Clarke,⁵⁴ M.E. Convery,¹⁵ J. Conway,⁷ M. Corbo,¹⁵ M. Cordelli,¹⁷ C.A. Cox,⁷ D.J. Cox,⁷ M. Cremonesi,⁴² D. Cruz,⁴⁸ J. Cuevas^z,⁹ R. Culbertson,¹⁵ N. d'Ascenzo^w,¹⁵ M. Datta^{qq},¹⁵ P. De Barbaro,⁴⁵ L. Demortier,⁴⁶ M. Deninno,⁶ F. Devoto,²¹ M. d'Errico^{ff},⁴⁰ A. Di Canto^{gg},⁴² B. Di Ruzza^q,¹⁵ J.R. Dittmann,⁵ M. D'Onofrio,²⁷ S. Donati^{gg},⁴² M. Dorigoⁿⁿ,⁴⁹ A. Driutti,⁴⁹ K. Ebina,⁵³ R. Edgar,³² A. Elagin,⁴⁸ R. Erbacher,⁷ S. Errede,²² B. Esham,²² R. Eusebi,⁴⁸ S. Farrington,³⁹ J.P. Fernández Ramos,²⁹ R. Field,¹⁶ G. Flanagan^u,¹⁵ R. Forrest,⁷ M. Franklin,²⁰ J.C. Freeman,¹⁵ H. Frisch,¹¹ Y. Funakoshi,⁵³ A.F. Garfinkel,⁴⁴ P. Garosi^{hh},⁴² H. Gerberich,²² E. Gerchtein,¹⁵ S. Giagu,⁴⁷ V. Giakoumopoulou,³ K. Gibson,⁴³ C.M. Ginsburg,¹⁵ N. Giokaris,³ P. Giromini,¹⁷ G. Giurgiu,²³ V. Glagolev,¹³ D. Glenzinski,¹⁵ M. Gold,³⁵ D. Goldin,⁴⁸ A. Golossanov,¹⁵ G. Gomez,⁹ G. Gomez-Ceballos,³⁰ M. Goncharov,³⁰ O. González López,²⁹ I. Gorelov,³⁵ A.T. Goshaw,¹⁴ K. Goulianos,⁴⁶ E. Gramellini,⁶ S. Grinstein,⁴ C. Grosso-Pilcher,¹¹ R.C. Group^{52,15} J. Guimaraes da Costa,²⁰ S.R. Hahn,¹⁵ J.Y. Han,⁴⁵ F. Happacher,¹⁷ K. Hara,⁵⁰ M. Hare,⁵¹ R.F. Harr,⁵⁴ T. Harrington-Taberⁿ,¹⁵ K. Hatakeyama,⁵ C. Hays,³⁹ J. Heinrich,⁴¹ M. Herndon,⁵⁵ A. Hocker,¹⁵ Z. Hong,⁴⁸ W. Hopkins^g,¹⁵ S. Hou,¹ R.E. Hughes,³⁶ U. Husemann,⁵⁶ M. Hussein,³³ J. Huston,³³ G. Introzzi^{mm},⁴² M. Iori^{jj},⁴⁷ A. Ivanov^p,⁷ E. James,¹⁵ D. Jang,¹⁰ B. Jayatilaka,¹⁵ E.J. Jeon,²⁵ S. Jindariani,¹⁵ M. Jones,⁴⁴ K.K. Joo,²⁵ S.Y. Jun,¹⁰ T.R. Junk,¹⁵ M. Kambeitz,²⁴ T. Kamon^{25,48} P.E. Karchin,⁵⁴ A. Kasmi,⁵ Y. Kato^o,³⁸ W. Ketchum^{rr},¹¹ J. Keung,⁴¹ B. Kilminster^{oo},¹⁵ D.H. Kim,²⁵ H.S. Kim,²⁵ J.E. Kim,²⁵ M.J. Kim,¹⁷ S.B. Kim,²⁵ S.H. Kim,⁵⁰ Y.K. Kim,¹¹ Y.J. Kim,²⁵ N. Kimura,⁵³ M. Kirby,¹⁵ K. Knoepfel,¹⁵ K. Kondo^{*},⁵³ D.J. Kong,²⁵ J. Konigsberg,¹⁶ A.V. Kotwal,¹⁴ M. Kreps,²⁴ J. Kroll,⁴¹ M. Kruse,¹⁴ T. Kuhr,²⁴ M. Kurata,⁵⁰ A.T. Laasanen,⁴⁴ S. Lammel,¹⁵ M. Lancaster,²⁸ K. Lannon^y,³⁶ G. Latino^{hh},⁴² H.S. Lee,²⁵ J.S. Lee,²⁵ S. Leo,⁴² S. Leone,⁴² J.D. Lewis,¹⁵ A. Limosani^t,¹⁴ E. Lipeles,⁴¹ H. Liu,⁵² Q. Liu,⁴⁴ T. Liu,¹⁵ S. Lockwitz,⁵⁶ A. Loginov,⁵⁶ D. Lucchesi^{ff},⁴⁰ J. Lueck,²⁴ P. Lujan,²⁶ P. Lukens,¹⁵ G. Lungu,⁴⁶ J. Lys,²⁶ R. Lysak^e,¹² R. Madrak,¹⁵ P. Maestro^{hh},⁴² S. Malik,⁴⁶ G. Manca^a,²⁷ A. Manousakis-Katsikakis,³ F. Margaroli,⁴⁷ P. Marinoⁱⁱ,⁴² M. Martínez,⁴ K. Matera,²² M.E. Mattson,⁵⁴ A. Mazzacane,¹⁵ P. Mazzanti,⁶ R. McNulty^j,²⁷ A. Mehta,²⁷ P. Mehtala,²¹ C. Mesropian,⁴⁶ T. Miao,¹⁵ D. Mietlicki,³² A. Mitra,¹ H. Miyake,⁵⁰ S. Moed,¹⁵ N. Moggi,⁶ C.S. Moon^{aa},¹⁵ R. Moore^{pp},¹⁵ M.J. Morelloⁱⁱ,⁴² A. Mukherjee,¹⁵ Th. Muller,²⁴ P. Murat,¹⁵ M. Mussini^{ee},⁶ J. Nachtmanⁿ,¹⁵ Y. Nagai,⁵⁰ J. Naganoma,⁵³ I. Nakano,³⁷ A. Napier,⁵¹ J. Nett,⁴⁸ C. Neu,⁵² T. Nigmanov,⁴³ L. Nodulman,² S.Y. Noh,²⁵ O. Norniella,²² L. Oakes,³⁹ S.H. Oh,¹⁴ Y.D. Oh,²⁵ I. Oksuzian,⁵² T. Okusawa,³⁸ R. Orava,²¹ L. Ortolan,⁴ C. Pagliarone,⁴⁹ E. Palencia^f,⁹ P. Palni,³⁵ V. Papadimitriou,¹⁵ W. Parker,⁵⁵ G. Pauletta^{kk},⁴⁹ M. Paulini,¹⁰ C. Paus,³⁰ T.J. Phillips,¹⁴ G. Piacentino,⁴² E. Pianori,⁴¹ J. Pilot,³⁶ K. Pitts,²² C. Plager,⁸ L. Pondrom,⁵⁵ S. Poprocki^g,¹⁵ K. Potamianos,²⁶ F. Prokoshin^{cc},¹³ A. Pranko,²⁶ F. Ptohos^h,¹⁷ G. Punzi^{gg},⁴² N. Ranjan,⁴⁴ I. Redondo Fernández,²⁹ P. Renton,³⁹ M. Rescigno,⁴⁷ T. Riddick,²⁸ F. Rimondi^{*},⁶ L. Ristori^{42,15} A. Robson,¹⁹ T. Rodriguez,⁴¹ S. Rolliⁱ,⁵¹ M. Ronzani^{gg},⁴² R. Roser,¹⁵ J.L. Rosner,¹¹ F. Ruffini^{hh},⁴² A. Ruiz,⁹ J. Russ,¹⁰ V. Rusu,¹⁵ A. Safonov,⁴⁸ W.K. Sakumoto,⁴⁵ Y. Sakurai,⁵³ L. Santi^{kk},⁴⁹ K. Sato,⁵⁰ V. Saveliev^w,¹⁵ A. Savoy-Navarro^{aa},¹⁵ P. Schlabach,¹⁵ E.E. Schmidt,¹⁵ T. Schwarz,³² L. Scodellaro,⁹ F. Scuri,⁴² S. Seidel,³⁵ Y. Seiya,³⁸ A. Semenov,¹³ F. Sforza^{gg},⁴² S.Z. Shalhout,⁷ T. Shears,²⁷ P.F. Shepard,⁴³ M. Shimojima^v,⁵⁰ M. Shochet,¹¹ I. Shreyber-Tecker,³⁴ A. Simonenko,¹³ P. Sinervo,³¹ K. Sliwa,⁵¹ J.R. Smith,⁷ F.D. Snider,¹⁵ V. Sorin,⁴ H. Song,⁴³ M. Stancari,¹⁵ R. St. Denis,¹⁹ B. Stelzer,³¹ O. Stelzer-Chilton,³¹ D. Stentz^x,¹⁵ J. Strologas,³⁵ Y. Sudo,⁵⁰ A. Sukhanov,¹⁵ I. Suslov,¹³ K. Takemasa,⁵⁰ Y. Takeuchi,⁵⁰ J. Tang,¹¹ M. Tecchio,³² P.K. Teng,¹ J. Thom^g,¹⁵

E. Thomson,⁴¹ V. Thukral,⁴⁸ D. Toback,⁴⁸ S. Tokar,¹² K. Tollefson,³³ T. Tomura,⁵⁰ D. Tonelli,^{f,15} S. Torre,¹⁷ D. Torretta,¹⁵ P. Totaro,⁴⁰ M. Trovato,^{ii,42} F. Ukegawa,⁵⁰ S. Uozumi,²⁵ F. Vázquez,^{m,16} G. Velev,¹⁵ C. Vellidis,¹⁵ C. Vernieri,^{ii,42} M. Vidal,⁴⁴ R. Vilar,⁹ J. Vizán,^{ii,9} M. Vogel,³⁵ G. Volpi,¹⁷ P. Wagner,⁴¹ R. Wallny,⁸ S.M. Wang,¹ A. Warburton,³¹ D. Waters,²⁸ W.C. Wester III,¹⁵ D. Whiteson,^{b,41} A.B. Wicklund,² S. Wilbur,¹¹ H.H. Williams,⁴¹ J.S. Wilson,³² P. Wilson,¹⁵ B.L. Winer,³⁶ P. Wittich,^{g,15} S. Wolbers,¹⁵ H. Wolfe,³⁶ T. Wright,³² X. Wu,¹⁸ Z. Wu,⁵ K. Yamamoto,³⁸ D. Yamato,³⁸ T. Yang,¹⁵ U.K. Yang,^{r,11} Y.C. Yang,²⁵ W.-M. Yao,²⁶ G.P. Yeh,¹⁵ K. Yi,^{n,15} J. Yoh,¹⁵ K. Yorita,⁵³ T. Yoshida,^{l,38} G.B. Yu,¹⁴ I. Yu,²⁵ A.M. Zanetti,⁴⁹ Y. Zeng,¹⁴ C. Zhou,¹⁴ and S. Zucchelli^{ee6}

(CDF Collaboration[†])

¹*Institute of Physics, Academia Sinica, Taipei, Taiwan 11529, Republic of China*

²*Argonne National Laboratory, Argonne, Illinois 60439, USA*

³*University of Athens, 157 71 Athens, Greece*

⁴*Institut de Física d'Altes Energies, ICREA, Universitat Autònoma de Barcelona, E-08193, Bellaterra (Barcelona), Spain*

⁵*Baylor University, Waco, Texas 76798, USA*

⁶*Istituto Nazionale di Fisica Nucleare Bologna, ^{ee}University of Bologna, I-40127 Bologna, Italy*

⁷*University of California, Davis, Davis, California 95616, USA*

⁸*University of California, Los Angeles, Los Angeles, California 90024, USA*

⁹*Instituto de Física de Cantabria, CSIC-University of Cantabria, 39005 Santander, Spain*

¹⁰*Carnegie Mellon University, Pittsburgh, Pennsylvania 15213, USA*

¹¹*Enrico Fermi Institute, University of Chicago, Chicago, Illinois 60637, USA*

¹²*Comenius University, 842 48 Bratislava, Slovakia; Institute of Experimental Physics, 040 01 Kosice, Slovakia*

¹³*Joint Institute for Nuclear Research, RU-141980 Dubna, Russia*

¹⁴*Duke University, Durham, North Carolina 27708, USA*

¹⁵*Fermi National Accelerator Laboratory, Batavia, Illinois 60510, USA*

¹⁶*University of Florida, Gainesville, Florida 32611, USA*

¹⁷*Laboratori Nazionali di Frascati, Istituto Nazionale di Fisica Nucleare, I-00044 Frascati, Italy*

¹⁸*University of Geneva, CH-1211 Geneva 4, Switzerland*

¹⁹*Glasgow University, Glasgow G12 8QQ, United Kingdom*

²⁰*Harvard University, Cambridge, Massachusetts 02138, USA*

²¹*Division of High Energy Physics, Department of Physics,*

University of Helsinki and Helsinki Institute of Physics, FIN-00014, Helsinki, Finland

²²*University of Illinois, Urbana, Illinois 61801, USA*

²³*The Johns Hopkins University, Baltimore, Maryland 21218, USA*

²⁴*Institut für Experimentelle Kernphysik, Karlsruhe Institute of Technology, D-76131 Karlsruhe, Germany*

²⁵*Center for High Energy Physics: Kyungpook National University,*

Daegu 702-701, Korea; Seoul National University, Seoul 151-742,

Korea; Sungkyunkwan University, Suwon 440-746,

Korea; Korea Institute of Science and Technology Information,

Daejeon 305-806, Korea; Chonnam National University,

Gwangju 500-757, Korea; Chonbuk National University, Jeonju 561-756,

Korea; Ewha Womans University, Seoul, 120-750, Korea

²⁶*Ernest Orlando Lawrence Berkeley National Laboratory, Berkeley, California 94720, USA*

²⁷*University of Liverpool, Liverpool L69 7ZE, United Kingdom*

²⁸*University College London, London WC1E 6BT, United Kingdom*

²⁹*Centro de Investigaciones Energeticas Medioambientales y Tecnológicas, E-28040 Madrid, Spain*

³⁰*Massachusetts Institute of Technology, Cambridge, Massachusetts 02139, USA*

³¹*Institute of Particle Physics: McGill University, Montréal, Québec H3A 2T8,*

Canada; Simon Fraser University, Burnaby, British Columbia V5A 1S6,

Canada; University of Toronto, Toronto, Ontario M5S 1A7,

Canada; and TRIUMF, Vancouver, British Columbia V6T 2A3, Canada

³²*University of Michigan, Ann Arbor, Michigan 48109, USA*

³³*Michigan State University, East Lansing, Michigan 48824, USA*

³⁴*Institution for Theoretical and Experimental Physics, ITEP, Moscow 117259, Russia*

³⁵*University of New Mexico, Albuquerque, New Mexico 87131, USA*

³⁶*The Ohio State University, Columbus, Ohio 43210, USA*

³⁷*Okayama University, Okayama 700-8530, Japan*

³⁸*Osaka City University, Osaka 588, Japan*

³⁹*University of Oxford, Oxford OX1 3RH, United Kingdom*

⁴⁰*Istituto Nazionale di Fisica Nucleare, Sezione di Padova-Trento, ^{ff}University of Padova, I-35131 Padova, Italy*

⁴¹*University of Pennsylvania, Philadelphia, Pennsylvania 19104, USA*

- ⁴²*Istituto Nazionale di Fisica Nucleare Pisa*, ⁹⁹*University of Pisa*,
^{hh}*University of Siena* and ⁱⁱ*Scuola Normale Superiore, I-56127 Pisa*,
Italy, ^{mm}*INFN Pavia and University of Pavia, I-27100 Pavia, Italy*
⁴³*University of Pittsburgh, Pittsburgh, Pennsylvania 15260, USA*
⁴⁴*Purdue University, West Lafayette, Indiana 47907, USA*
⁴⁵*University of Rochester, Rochester, New York 14627, USA*
⁴⁶*The Rockefeller University, New York, New York 10065, USA*
⁴⁷*Istituto Nazionale di Fisica Nucleare, Sezione di Roma 1*,
^{jj}*Sapienza Università di Roma, I-00185 Roma, Italy*
⁴⁸*Texas A&M University, College Station, Texas 77843, USA*
⁴⁹*Istituto Nazionale di Fisica Nucleare Trieste/Udine; ⁿⁿUniversity of Trieste*,
I-34127 Trieste, Italy; ^{kk}*University of Udine, I-33100 Udine, Italy*
⁵⁰*University of Tsukuba, Tsukuba, Ibaraki 305, Japan*
⁵¹*Tufts University, Medford, Massachusetts 02155, USA*
⁵²*University of Virginia, Charlottesville, Virginia 22906, USA*
⁵³*Waseda University, Tokyo 169, Japan*
⁵⁴*Wayne State University, Detroit, Michigan 48201, USA*
⁵⁵*University of Wisconsin, Madison, Wisconsin 53706, USA*
⁵⁶*Yale University, New Haven, Connecticut 06520, USA*
⁵⁷*University of California Irvine, Irvine, CA 92697, USA*

We present a search for the pair-production of a non-standard-model strongly-interacting particle that decays to a pair of quarks or gluons, leading to a final state with four hadronic jets. We consider both non-resonant production via an intermediate gluon as well as resonant production via a distinct non-standard-model intermediate strongly-interacting particle. We use data collected by the CDF experiment in proton-antiproton collisions at $\sqrt{s} = 1.96$ TeV corresponding to an integrated luminosity of 6.6 fb^{-1} . We find the data to be consistent with standard model predictions. We report limits on $\sigma(p\bar{p} \rightarrow jjjj)$ as a function of the masses of the hypothetical intermediate particles. Upper limits on the production cross sections for non-standard-model particles in several resonant and non-resonant processes are also derived.

PACS numbers:

*Deceased

†With visitors from ^a*Istituto Nazionale di Fisica Nucleare, Sezione di Cagliari, 09042 Monserrato (Cagliari), Italy*, ^b*University of California Irvine, Irvine, CA 92697, USA*, ^c*Institute of Physics, Academy of Sciences of the Czech Republic, 182 21, Czech Republic*, ^f*CERN, CH-1211 Geneva, Switzerland*, ^g*Cornell University, Ithaca, NY 14853, USA*, ^h*University of Cyprus, Nicosia CY-1678, Cyprus*, ⁱ*Office of Science, U.S. Department of Energy, Washington, DC 20585, USA*, ^j*University College Dublin, Dublin 4, Ireland*, ^k*ETH, 8092 Zürich, Switzerland*, ^l*University of Fukui, Fukui City, Fukui Prefecture, Japan 910-0017*, ^m*Universidad Iberoamericana, Lomas de Santa Fe, México, C.P. 01219, Distrito Federal*, ⁿ*University of Iowa, Iowa City, IA 52242, USA*, ^o*Kinki University, Higashi-Osaka City, Japan 577-8502*, ^p*Kansas State University, Manhattan, KS 66506, USA*, ^q*Brookhaven National Laboratory, Upton, NY 11973, USA*, ^r*University of Manchester, Manchester M13 9PL, United Kingdom*, ^s*Queen Mary, University of London, London, E1 4NS, United Kingdom*, ^t*University of Melbourne, Victoria 3010, Australia*, ^u*Muons, Inc., Batavia, IL 60510, USA*, ^v*Nagasaki Institute of Applied Science, Nagasaki 851-0193, Japan*, ^w*National Research Nuclear University, Moscow 115409, Russia*, ^x*Northwestern University, Evanston, IL 60208, USA*, ^y*University of Notre Dame, Notre Dame, IN 46556, USA*, ^z*Universidad de Oviedo, E-33007 Oviedo, Spain*, ^{aa}*CNRS-IN2P3, Paris, F-75205 France*, ^{cc}*Universidad Tecnica Federico Santa Maria, 110v Valparaiso, Chile*, ^{dd}*Yarmouk University, Irbid 211-63, Jordan*, ^{ll}*Universite catholique de Louvain, 1348 Louvain-La-Neuve, Belgium*, ^{oo}*University of Zürich, 8006 Zürich, Switzerland*, ^{pp}*Massachusetts General Hospital and Harvard Medical School, Boston, MA 02114 USA*, ^{qq}*Hampton University, Hampton, VA*

One of the few hints of possible physics beyond the standard model (SM) at the TeV scale is the anomalous top-quark forward-backward asymmetry A_{fb} observed at the Tevatron [1–3]. This asymmetry could be generated by non-SM physics through the production of top-quark pairs via a light axi-gluon [4], a particle with axial couplings to quarks, that interferes with standard model (SM) $t\bar{t}$ production to produce the observed asymmetry. The axi-gluon would be visible in its alternate decay mode to low-mass strongly-interacting particles, each of which decays to a pair of jets [5] yielding a four-jet final state. This final state is of broad interest, as various models predict pair-production of strongly-interacting particles decaying to jet pairs with no intermediate resonance [6, 7] and R -parity-violating supersymmetric theories [8] predict pair-production of light partners of the top quark (stop quarks), each decaying into to pairs of light quarks.

The masses of the axi-gluon and its strongly-interacting decay products are not predicted, but must be fairly light ($< 400 \text{ GeV}/c^2$) to explain the A_{fb} measurement [9]. The LHC experiments have excellent sensitivity

23668, USA, ^{rr}*Los Alamos National Laboratory, Los Alamos, NM 87544, USA*

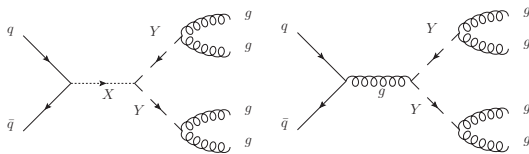


FIG. 1: Diagrams for resonant (left, via X) and non-resonant (right) pair-production of Y particles, with subsequent decays to pairs of gluons. Other models, with final-state quarks, are also considered.

at high mass due to the large center-of-mass energy, but difficulties at low mass due to high background rates. The ATLAS experiment ruled out masses between 100 and 150 GeV/c^2 [10]; CMS ruled out masses between 250 and 740 GeV/c^2 [11]. No experimental bounds exist for such non-SM particles with masses below 100 GeV/c^2 for non-resonant pair-production of di-jet resonances; there are no current limits on resonant production.

In this Letter we report a search for both non-resonant and resonant production of pairs of strongly-interacting particles, each of which decays to a pair of jets. Rather than probing a specific theory, we construct a simplified model with the minimal particle content. In the non-resonant case, we consider the production process $p\bar{p} \rightarrow YY \rightarrow jj\, jj$, with the mass of the hypothetical Y state, m_Y as a single free parameter. In the resonant case, $p\bar{p} \rightarrow X \rightarrow YY \rightarrow jj\, jj$, we also explore the mass of the X state, m_X (Fig. 1). In both cases, we assume that the natural width of the particles is small compared to the experimental resolution.

We analyze a sample of events corresponding to an integrated luminosity of $6.6 \pm 0.5 \text{ fb}^{-1}$ recorded by the CDF II detector [12], a general purpose detector designed to study $p\bar{p}$ collisions at $\sqrt{s} = 1.96 \text{ TeV}$ produced by the Fermilab Tevatron collider. The tracking system consists of a silicon microstrip tracker and a drift chamber immersed in a 1.4 T axial magnetic field [13]. Electromagnetic and hadronic calorimeters surrounding the tracking system measure particle energies, with muon detection provided by an additional system of drift chambers located outside the calorimeters.

We reconstruct jets in the calorimeter using the JET-CLU [14] algorithm with a clustering radius of 0.4 in $\eta - \phi$ space [15], and calibrated using the techniques outlined in Ref. [16]. Events are selected online (triggered) by the requirement of three jets, each with $E_T > 20 \text{ GeV}$ and with $\Sigma_{\text{jets}} E_T > 130 \text{ GeV}$ [15]. The data set used in this search is limited to 6.6 fb^{-1} because the trigger selection was not available in early data. After trigger selection, events are retained if at least four jets are found with $E_T > 15 \text{ GeV}$ and $|\eta| < 2.4$.

We model resonant and non-resonant production with MADGRAPH5 [17] version 1.4.8.4 and the CTEQ6L1 [18] parton distribution functions (PDF). Additional parton

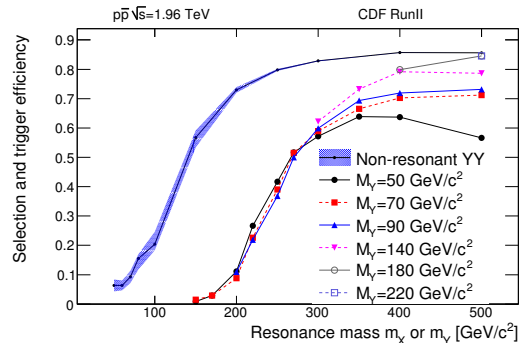


FIG. 2: Overall efficiency, including trigger and selection requirements. Efficiency is shown for several simulated non-resonant $YY \rightarrow jj\, jj$ samples with varying m_Y . The shaded band shows the uncertainty. Efficiency is shown for several simulated resonant $X \rightarrow YY \rightarrow jj\, jj$ samples with varying m_X and m_Y . The uncertainty is not shown but is similar to the non-resonant case. The turn-on curve is determined largely by the trigger requirement that $\Sigma_{\text{jets}} E_T > 130 \text{ GeV}$.

radiation, hadronization, and underlying-event modeling are described by PYTHIA [19] version 6.420. The detector response for all simulated samples is modeled by the GEANT-based CDF II detector simulation [20].

The trigger and selection requirements have an efficiency on the signal up to 90% if $\Sigma_{\text{jets}} E_T$ exceeds significantly the 130 GeV trigger threshold. For events with smaller $\Sigma_{\text{jets}} E_T$, the efficiency decreases rapidly (Fig. 2). In the non-resonant-production model, the $\Sigma_{\text{jets}} E_T$ is strongly correlated with m_Y . In the resonant-production model it is correlated with m_X ; additionally if $m_X - 2m_Y$ is large, the p_T of the resulting Y is large, which leads to a small opening angle of its decay products and a loss of efficiency due to merged jets. The trigger efficiency is measured in simulated events, and uncertainties derived from validation in disjoint samples; the measured trigger efficiency and uncertainty are applied to the signal model.

To reconstruct the di-jet resonance, we consider the four leading jets and evaluate the invariant mass of each of the di-jet pairs in the three permutations, choosing the permutation with the smallest mass difference between the pairs. As the pair masses are correlated, we take the mean of the two pair masses as the estimate of the di-jet resonance mass. To reduce backgrounds, we require that the relative mass difference between the two pairs is less than 50%, and that the production angle θ^* of the di-jet resonance in the YY pair center-of-mass frame satisfies $\cos(\theta^*) < 0.9$. In the resonant production analysis, we calculate the four-jet invariant mass. No specific m_Y -dependent selections are made; the requirement that the relative di-jet mass difference be small ensures compatibility with the $X \rightarrow YY$ hypothesis. Figures 3 and 4 show the observed di-jet and four-jet spectra, re-

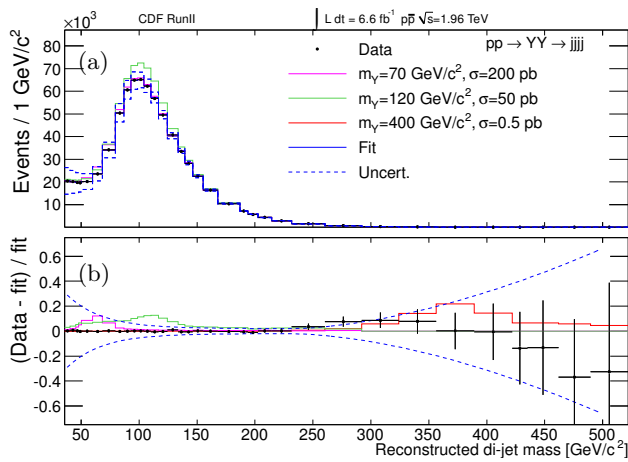


FIG. 3: Reconstructed mean di-jet mass in events with four jets. Parametric fit and several signal hypotheses overlaid in (a). Relative difference between the observed data and the fit in each bin shown in (b).

spectively.

The dominant background originates from standard QCD multi-jet production. We model this background contribution using a parametric function which is fit to the reconstructed mass spectrum of the observed data. The function is a piece-wise combination of a third-order polynomial to describe the turn-on region, a third-order polynomial to describe the peak region, and a double exponential of the form $f(m) = a_1 e^{-(m-a_2)^{a_3}/a_4}$ to describe the falling spectrum. The parametric functional form was chosen to be flexible enough to describe the multi-jet mass spectrum, but rigid enough to avoid accurately describing a spectrum which includes a narrow resonance, so that in the presence of a narrow feature a signal-plus-background hypothesis would be preferred. For the di-jet mass, the ranges used are [35, 82.5], [82.5, 140], and [140, 700] GeV/c^2 ; for the four-jet mass, the ranges used are [115, 185], [185, 330], and [330, 800] GeV/c^2 . The functional form and ranges were chosen based on their ability to accurately describe the mass spectra of simulated multi-jet events generated by ALPGEN [21] version 2.10.

The dominant source of systematic uncertainty is due to the multi-jet background model. The functional form is an approximation, which even in the absence of a narrow feature may deviate from the observed spectrum. We estimate the impact of these potential deviations by measuring their magnitude in two background-enriched control samples. These two control samples are adjacent to the signal region and capture the expected deviations in two independent directions. The first requires a large relative di-jet mass difference, greater than 50%, and the second requires $\cos(\theta^*) > 0.9$. The observed relative deviations are then applied to the observed spectrum in the signal region to estimate the magnitude of spurious

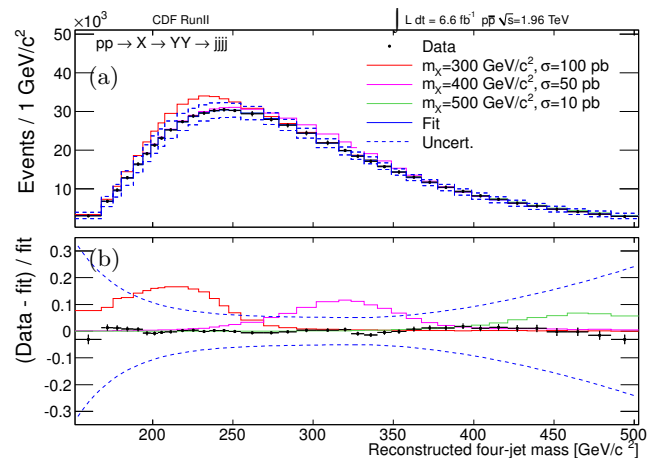


FIG. 4: Reconstructed four-jet mass in events with four jets. Parametric fit and several signal hypotheses overlaid in (a). Relative difference between the observed data and the fit in each bin shown in (b).

deviations due to possible mismodeling. In addition, we verify that the fitting procedure gives an unbiased estimate of the signal rate.

An additional uncertainty is due to knowledge of the trigger efficiency [22] extracted from the simulated signal samples, varying from 20% relative at $\Sigma_{\text{jets}} E_T = 120$ GeV to 10% above $\Sigma_{\text{jets}} E_T = 200$ GeV. Uncertainties in the levels of parton radiation [23] and in the calibration of the jet energy and resolution modeling [16] also contribute to uncertainties in the trigger and selection efficiency and reconstructed mass spectrum of the signal samples. These uncertainties are small ($< 10\%$) relative to the fitting and trigger uncertainties.

In the non-resonant analysis, for each Y mass hypothesis, we fit the most likely value of the Y pair-production cross section (σ_{YY}) by performing a maximum likelihood fit of the binned di-jet mass distribution, allowing for systematic and statistical fluctuations via template morphing [24]. The likelihood takes the form of

$$L(\sigma_{YY}) = \prod_{\text{bin } i} f_{\text{bg}}^i(\vec{a}) + \sigma_{YY} \mathcal{L} \epsilon f_{\text{sig}},$$

where $f_{\text{bg}}(\vec{a})$ is the parametric function with nuisance parameters \vec{a} defined above to describe the background spectrum, f_{sig} is a normalized template of the expected shape of the signal determined from simulated events, and $\mathcal{L} \epsilon$ is the product of the integrated luminosity and efficiency. No evidence is found for the presence of pair-production of di-jet resonances and upper limits on Y pair-production at 95% confidence level (C.L.) are set.

Limits are calculated using the CLs [25] method by repeating the measurement on sets of simulated experiments that include signal contributions corresponding to various hypothetical production cross-sections, and variation of systematic uncertainties. The values of nu-

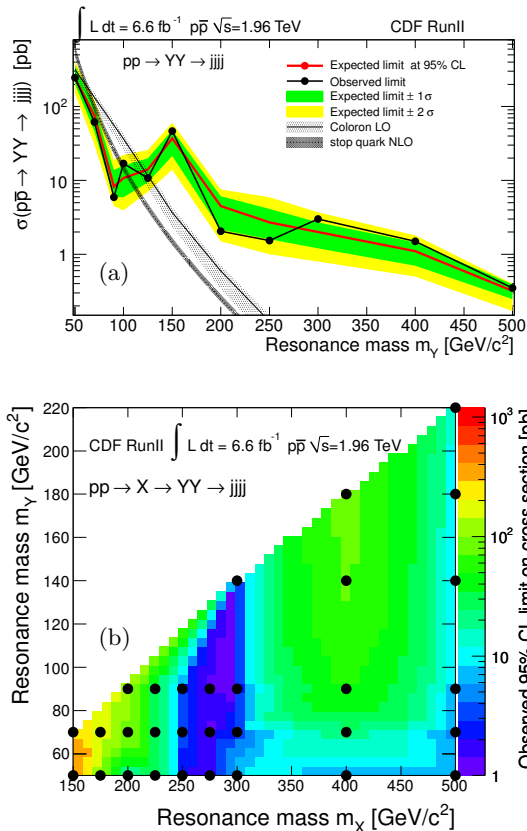


FIG. 5: Upper limit on signal production rate at 95% C.L. Expected and observed upper limits on $\sigma(pp \rightarrow YY \rightarrow jjjj)$ versus m_Y in the non-resonant analysis shown in (a). Two signal hypotheses are shown, see text for details. Observed limits on $\sigma(pp \rightarrow X \rightarrow YY \rightarrow jjjj)$ versus m_X and m_Y shown in (b). Circles indicate the true values of the parameters used in each ensemble of simulated samples used to evaluate the limits; intermediate values are interpolated.

sance parameters are not fit in the experiments. The observed limits are consistent with expectation for the background-only hypothesis. The resonant analysis is very similar, but is done as a function of the X mass hypothesis, fitting the four-jet mass distribution for the most likely value of X production cross section, σ_X .

In the non-resonant case, this analysis sets limits on coloron or stop-quark pair production, excluding 50-100 GeV/c^2 and 50-125 GeV/c^2 , respectively; see Table I and the top of Fig. 5. The uncertainty on the theoretical cross-section prediction comes from two sources summed in quadrature. The first uncertainty is the envelope of the PDF uncertainties from the CTEQ uncertainties and an alternative PDF choice, MSTW2008LO [26] (5% relative). The second uncertainty comes from a variation of the renormalization and factorization scales by a factor of two in each direction from their default values of the per-event mass scale. These theoretical uncertainties are illustrated in Figure 5.

In the resonant case, this analysis excludes axi-gluon (A) production leading to pairs of σ particles and four-

TABLE I: Observed and expected 95% C.L. upper limits on $\sigma(pp \rightarrow YY \rightarrow jj jj)$ for several values of m_Y . Also shown are theoretical predictions for coloron pair production [6, 7] or stop-quark pair production with R -parity-violating decay $\tilde{t} \rightarrow qq'$ [27].

Mass (GeV/c^2)	Expected (pb)	Observed (pb)	Coloron (pb)	Stop quarks (pb)
50	240	250	320	570
70	75	62	180	100
90	8.2	5.9	62	26
100	11	17	37	15
125	14	11	11	4.4
150	37	46	3.7	1.5
200	4.5	2.0	0.60	0.25
250	2.7	1.5	0.11	5.4×10^{-2}
300	2.0	3.0	2.9×10^{-2}	1.3×10^{-2}
400	1.1	1.5	1.7×10^{-3}	7.2×10^{-4}
500	0.3	0.3	8.5×10^{-5}	3.6×10^{-5}

TABLE II: Observed and expected 95% C.L. upper limits on $\sigma(pp \rightarrow X \rightarrow YY \rightarrow jj jj)$ for several values of m_Y and m_X . Also shown are theoretical predictions for axi-gluon production assuming coupling to quarks of $C_q = 0.4$ [5, 9].

m_X (GeV/c^2)	m_Y (GeV/c^2)	Expected (pb)	Observed (pb)	Axi-gluon (pb)
150	50	641.2	431.1	5600
	70	209.6	270.6	
175	50	66.8	78.9	3500
	70	111.5	163.9	
200	50	13.8	9.5	2200
	70	30.4	91.5	
	90	17.8	100.4	
225	50	18.0	26.0	1750
	70	20.7	25.0	
	90	20.9	25.3	
250	50	6.2	2.0	1000
	70	4.0	3.6	
	90	5.1	2.8	
275	50	6.5	1.2	850
	70	7.7	1.3	
	90	9.7	1.4	
300	50	5.0	7.1	540
	70	2.4	2.6	
	90	1.7	1.0	
	140	1.8	1.2	
400	50	15.5	6.8	170
	70	15.0	20.2	
	90	30.6	52.8	
	140	41.0	74.6	
	180	46.9	79.1	
500	50	20.7	6.8	60
	70	15.9	4.7	
	90	17.7	5.9	
	140	25.2	7.0	
	180	26.7	8.0	
	220	29.7	9.3	

gluon final state for $m_A \in [150, 400]$, $m_\sigma \in [50, m_A/2]$ in the case of coupling to quarks $C_q = 0.4$ (see Table II and the bottom of Fig. 5) which is close to the value required to explain the top-quark A_{fb} result [9]. To be consistent with this analysis, the couplings would have to be smaller by an order of magnitude. Maintaining consistency with the top-quark A_{fb} result would require different couplings to light quarks and heavy quarks, with the heavy-quark coupling approaching the perturbative limit, $C_q < 1$.

We thank Martin Schmaltz, Gustavo Tavares, Can Kilic, Bogdan Dobrescu, Dirk Zerwas and Felix Yu for useful suggestions and technical advice. We thank the Fermilab staff and the technical staffs of the participating institutions for their vital contributions. This work was supported by the U.S. Department of Energy and National Science Foundation; the Italian Istituto Nazionale di Fisica Nucleare; the Ministry of Education, Culture, Sports, Science and Technology of Japan; the Natural Sciences and Engineering Research Council of Canada; the National Science Council of the Republic of China; the Swiss National Science Foundation; the A.P. Sloan Foundation; the Bundesministerium für Bildung und Forschung, Germany; the Korean World Class University Program, the National Research Foundation of Korea; the Science and Technology Facilities Council and the Royal Society, UK; the Russian Foundation for Basic Research; the Ministerio de Ciencia e Innovación, and Programa Consolider-Ingenio 2010, Spain; the Slovak R&D Agency; the Academy of Finland; and the Australian Research Council (ARC).

-
- [1] T. Aaltonen *et al.* (CDF Collaboration), Phys. Rev. Lett. **101**, 202001 (2008).
- [2] V. M. Abazov *et al.* (D0 Collaboration), Phys. Rev. Lett. **100**, 142002 (2008).
- [3] T. Aaltonen *et al.* (CDF Collaboration), Phys. Rev. D **83**, 112003 (2011).
- [4] P. H. Frampton and S. L. Glashow, Phys. Lett. B **190**, 157 (1987).
- [5] G. Marques Tavares and M. Schmaltz, Phys. Rev. D **84**, 054008 (2011).
- [6] Y. Bai and B. A. Dobrescu, J. High Energy Phys. **07** (2011) 100.
- [7] C. Kilic, T. Okui, and R. Sundrum, J. High Energy Phys. **07** (2008) 038; C. Kilic, S. Schumann, and M. Son, J. High Energy Phys. **04** (2009) 128.
- [8] S. P. Martin, In Kane, G.L. (ed.): *Perspectives on supersymmetry II* 1-153 (1997).
- [9] C. Gross, G. Marques Tavares, C. Spethmann, and M. Schmaltz, arXiv:1209.6375 [hep-ph] (2012).
- [10] G. Aad *et al.* (ATLAS Collaboration), Eur. Phys. J. C **71**, 1828 (2011).
- [11] S. Chatrchyan *et al.* (CMS Collaboration), arXiv:1302.0531 [hep-ex] (2012).
- [12] T. Aaltonen *et al.* (CDF Collaboration), Phys. Rev. D **71**, 032001 (2005).
- [13] C. S. Hill, Nucl. Instrum. Methods A **530**, 1 (2004).
- [14] T. Aaltonen *et al.* (CDF Collaboration), Phys. Rev. D **45**, 001448 (1992).
- [15] CDF uses a cylindrical coordinate system with the z axis along the proton beam axis. For a particle or a jet, pseudorapidity is $\eta \equiv -\ln[\tan(\theta/2)]$, where θ is the polar angle relative to the proton beam direction, and ϕ is the azimuthal angle while transverse momentum $p_T = |p| \sin \theta$, and the transverse energy $E_T = E \sin \theta$.
- [16] A. Bhatti *et al.*, Nucl. Instrum. Methods A **566**, 375 (2006).
- [17] J. Alwall, P. Demin, S. de Visscher, R. Frederix, M. Herquet, F. Maltoni, T. Plehn, D. L. Rainwater, and T. Stelzer, J. High Energy Phys. **09** (2007) 028.
- [18] J. Pumplin *et al.* (CTEQ Collaboration), J. High. Energy Phys. **07** (2002) 012.
- [19] T. Sjostrand *et al.*, Comput. Phys. Commun. **238**, 135 (2001), version 6.422.
- [20] E. Gerchtein and M. Paulini, arXiv:physics/0306031 (2003).
- [21] M. L. Mangano, M. Moretti, F. Piccinini, R. Pittau, and A. D. Polosa, J. High Energy Phys. **07** (2003) 001.
- [22] T. Aaltonen *et al.* (CDF Collaboration), Phys. Rev. D **84**, 052010 (2011).
- [23] T. Aaltonen *et al.* (CDF Collaboration), Phys. Rev. D **73**, 032003 (2006).
- [24] A. Read, Nucl. Instrum. Methods A **425**, 357 (1999).
- [25] A. Read, J. Phys. G: Nucl. Part. Phys. **28**, 2693 (2002); T. Junk, Nucl. Instrum. Methods A **434**, 425 (1999).
- [26] A. D. Martin, W. J. Stirling, R. S. Thorne, and G. Watt, Eur. Phys. J. C **63**, 189 (2009).
- [27] W. Beenakker, M. Kramer, T. Plehn, M. Spira, and P. M. Zerwas, Nucl. Phys. **B515**, 3 (1998).